

## Test of single cluster update for the three-dimensional $XY$ model

W. Janke

*Institut für Theorie der Elementarteilchen, Freie Universität Berlin, Arnimallee 14, D-1000 Berlin 33, Germany*

Received 6 June 1990; accepted for publication 20 June 1990

Communicated by A.A. Maradudin

The Monte Carlo cluster update in Wolff's single cluster formulation is tested for the three-dimensional  $XY$  model on simple cubic lattices. A significant reduction of critical slowing down near the phase transition is observed. Combined with the use of improved estimators and histogram sampling, this allows accurate computations of the transition temperature and the critical exponents in reasonable computer time.

It is well known that importance sampling Monte Carlo (MC) algorithms based on local update schemes suffer near a phase transition from so-called "critical slowing down" [1]. By this one means that successive configurations are strongly correlated with a correlation time  $\tau \propto L^z$  ( $z \approx 2$  and  $L$  is the linear size of the system) and cannot be used for statistically independent measurements. Consequently, for fixed finite computer budget, the available statistics and thus the accuracy of the data are dramatically reduced in the most interesting regions of a phase diagram. Apart from overrelaxation [2] and multigrid [3] ideas, this problem has recently been overcome by means of physically very appealing global update algorithms in which whole clusters are updated in a coherent way [4,5]. It is intuitively clear that this leads to a much more efficient sampling of long wavelength fluctuations than in local update schemes. Currently there are two related formulations available. First, the Swendsen-Wang (SW) [4] formulation, in which the whole lattice is decomposed into clusters, and second, Wolff's [5] formulation, which is based on the generation of a single cluster in each step. Tests of these cluster algorithms for two-dimensional  $O(n)$  ( $n=1, 2, 3$ ) spin models [5-8] and the three-dimensional Ising model [9] have clearly demonstrated that critical slowing down is significantly reduced (with exponent  $z \ll 1$ ).

The purpose of this note is to report additional tests

of the *single cluster* (SC) formulation for a three-dimensional model with continuous symmetry, the  $XY$  (or  $O(2)$ ) model. The partition function is given by

$$Z = \prod_{\mathbf{x}} \left( \int_{-\pi}^{\pi} \frac{d\boldsymbol{\theta}(\mathbf{x})}{2\pi} \right) \exp(-\beta E), \quad (1)$$

where  $\beta \equiv 1/T$  is the (reduced) inverse temperature and the energy is

$$E = \sum_{\mathbf{x}, i} [1 - \mathbf{s}(\mathbf{x}) \cdot \mathbf{s}(\mathbf{x} + i)] \\ = \sum_{\mathbf{x}, i} \{1 - \cos[\nabla_i \boldsymbol{\theta}(\mathbf{x})]\}. \quad (2)$$

As usual  $\mathbf{s} = (\cos \boldsymbol{\theta}, \sin \boldsymbol{\theta})$  denote two-dimensional unit spins at the sites  $\mathbf{x}$  of a simple cubic lattice with periodic boundary conditions, and  $\nabla_i \boldsymbol{\theta} \equiv \boldsymbol{\theta}(\mathbf{x} + i) - \boldsymbol{\theta}(\mathbf{x})$  are the lattice gradients. It is well known that the three-dimensional  $XY$  model is the simplest lattice model [10] describing many properties of liquid helium and its  $\lambda$ -transition at  $T_\lambda = 2.18$  K [11] to the superfluid state. On the lattice, high-temperature series (HTS) analyses predict a continuous transition of this type at  $T_c^{\text{HTS}} = 2.203 \pm 0.006$  ( $\beta_c^{\text{HTS}} = 0.4539 \pm 0.0013$ ) [12]. It is also known that the lattice model can be rewritten in terms of line-like topological excitations which can be interpreted as vortex lines meandering through the superfluid helium at any non-zero temperature [13,14]. Ever since Onsager's [15] early comments and Feyn-

man's [16] more detailed analysis, there have been several attempts to understand the  $\lambda$ -transition as proliferation of these vortex lines or their lattice analogs [17]. Recently, phenomenological renormalization group ideas have been applied to the line representation [18,19], and it is clearly important to have precise MC data for comparison. Previous simulations using standard updates are much less accurate [20].

Initially we planned to perform a similar study also for the multiple cluster SW algorithm in order to compare the two new update schemes. Fortunately, after our single cluster update runs had essentially been completed, we received a preprint by Hasenbusch and Meyer [21], reporting tests of just this SW algorithm. Clearly, to avoid unnecessary duplication, we have used their data for the planned comparison.

In Wolff's single cluster formulation, one update consists of choosing (a) a random mirror direction and (b) a random site, which is the starting point for (c) growing a cluster of reflected spins. The size and shape of the cluster is controlled by a Metropolis-like accept/reject criterion, satisfying detailed balance [5]. Compared with the multiple cluster SW algorithm this formulation is technically somewhat simpler to implement, and, as we shall see below, numerically more efficient. The reason is that, on the average, larger clusters are moved.

To test its performance for the three-dimensional XY model, we have concentrated on the internal energy per site,  $e = \langle E \rangle / V$  ( $\langle \rangle$  denote thermal averages, and  $V = L^3$  is the lattice volume), and the susceptibility in the disordered state,

$$\chi = V \langle m^2 \rangle, \quad m = \frac{1}{V} \sum_x s(x), \quad (3)$$

and recorded the autocorrelation functions of these two observables,

$$A(k) = \frac{\langle O_i O_{i+k} \rangle - \langle O_i \rangle^2}{\langle O_i^2 \rangle - \langle O_i \rangle^2}. \quad (4)$$

Here  $O_i$  stands short for the  $i$ th measurement of  $E$  or  $m^2$ . Of practical importance is the integrated autocorrelation time

$$r \equiv \frac{1}{2} + \sum_{k=1}^{\infty} A(k), \quad (5)$$

which enters directly in the error estimate  $\epsilon$  for the mean of  $N$  correlated measurements with variance  $\sigma$ ,

$$\epsilon = \sqrt{\sigma^2 / N} \sqrt{2\tau}. \quad (6)$$

For completely uncorrelated measurements,  $A(k) = \delta_{k0}$  and  $\tau = \frac{1}{2}$ . Hence  $\sqrt{2\tau}$  measures directly the enhancement of statistical errors due to temporal correlations.

Clearly, in an actual simulation with finite running time, the summation in (5) must be cut off at a finite  $k = n$ , say, and some extrapolation procedure is needed. Assuming a purely exponential decay<sup>#1</sup> for  $k > k_0$ ,  $A(k) \approx a \exp(-k/\tau_0)$ , one readily finds for  $n \geq k_0$

$$\begin{aligned} \tau(n) &\equiv \frac{1}{2} + \sum_{k=1}^n A(k) \\ &= \tau - a \frac{\exp(-1/\tau_0)}{1 - \exp(-1/\tau_0)} \exp(-n/\tau_0) \end{aligned} \quad (7)$$

$$= \tau - \frac{A(n+1)}{1 - A(n+1)/A(n)}, \quad (8)$$

showing that

$$\tau(n) + \frac{A(n+1)}{1 - A(n+1)/A(n)}$$

is an improved extrapolant for  $\tau$  [9]. Alternatively, for  $n \geq k_0$ , one may simply employ a (non-linear) three-parameter fit of  $\tau(n)$  to the right-hand side of eq. (7) to determine  $\tau$ . A useful check is provided by the usual block averages and their associated errors which, for large blocks, should also approach (6) (but with different correction terms). As discussed previously [5], for the single cluster update some care is necessary in defining the unit of time, since in each update step only a relatively small fraction of the spins is moved, depending on temperature and lattice size. More precisely, our results show that, near  $T_c$  and for all lattice sizes, the average cluster size,  $\langle C \rangle$ , is proportional to the susceptibility,

$$\langle C \rangle \approx c\chi(L, T), \quad (9)$$

with  $c \approx 0.81$  (as in two dimensions [5]). At  $T_c$ , the susceptibility behaves like  $\chi \propto L^{\nu/\nu} = L^{2-\eta}$  (with very

<sup>#1</sup> For a bivariate Gaussian distribution with  $A(1) \equiv \rho \equiv \exp(-1/\tau_0)$  this is exactly valid for all  $k$  with  $a=1$ , and  $\tau = \frac{1}{2}(1+\rho)/(1-\rho) = \tau_0[1 + 1/12\tau_0^2 + O(1/\tau_0^4)]$ .

small  $\eta \approx 0.04$ ), so that with increasing lattice size the fraction of moved spins in each update step decreases like  $\langle C \rangle / V \propto L^{-(1+\eta)}$ , i.e., roughly  $\propto 1/L$ . Since the CPU time needed for a single cluster update is roughly proportional to the number of moved spins, it is appropriate to use  $N_0 \equiv V / \langle C \rangle \propto L^{1+\eta}$  single update steps as unit of time. This is then directly comparable with other update schemes that attempt moves for all spins in one update step. All our integrated autocorrelation times refer to this unit of time (which can always be achieved by a rescaling). Near  $T_c$ , with our Fortran program on a CRAY-XMP, the update of one spin took about 8–9  $\mu$ s.

Our first runs were performed at the HTS estimate,  $\beta \equiv \beta_c^{\text{HTS}} = 0.4539$  [12]. In fig. 1 the integrated autocorrelation times on a  $32^3$  lattice for energy and susceptibility,  $\tau_e$ ,  $\tau_\chi$ , are shown as thick vertical bars. The lengths of the vertical bars indicate the statistical errors which are estimated by dividing the whole run into five blocks, calculating  $\tau(n)$  in each of them, and taking the variance. In this run  $E$  and  $m^2$  were computed every 10th update step, corresponding on the average to  $0.284V$  moved spins between measurements. We have checked that increasing the interval between measurements to  $N_0 \approx 36$  steps, so that roughly all spins are moved, gives the same final results within the error bars. Fitting the data for  $n = 12, \dots, 32$  to the ansatz (7) (using the subroutine MRQMIN of ref. [22]), we find the solid interpolating curves. The resulting values of  $\tau_e$  and  $\tau_\chi$  (and their errors) are shown as the solid (dashed) horizontal lines at  $\tau_e \approx 3$  and  $\tau_\chi \approx 1.6$ , respectively. The crosses finally are the improved extrapolants for  $\tau_e$  and  $\tau_\chi$  according to eq. (8). We see that both methods are in very good agreement. Estimates of  $\tau$  based on the block errors mentioned above gave also always consistent results within 5%. Without any extrapolation procedure, however, they systematically underestimate  $\tau$ , as expected. Repeating such an analysis for various lattice sizes up to  $48^3$  at  $\beta_0 = 0.4539$  and  $\beta'_0 = 0.4543$ , we have determined the values for  $\tau_e$  and  $\tau_\chi$  shown in fig. 2. Obviously,  $\tau_\chi$  is essentially independent of  $L$ , and for all practical purposes we may conclude that

$$\tau_\chi \approx 1.7 = \text{const.} \quad (10)$$

While also small, the behaviour of  $\tau_e$  is clearly dif-

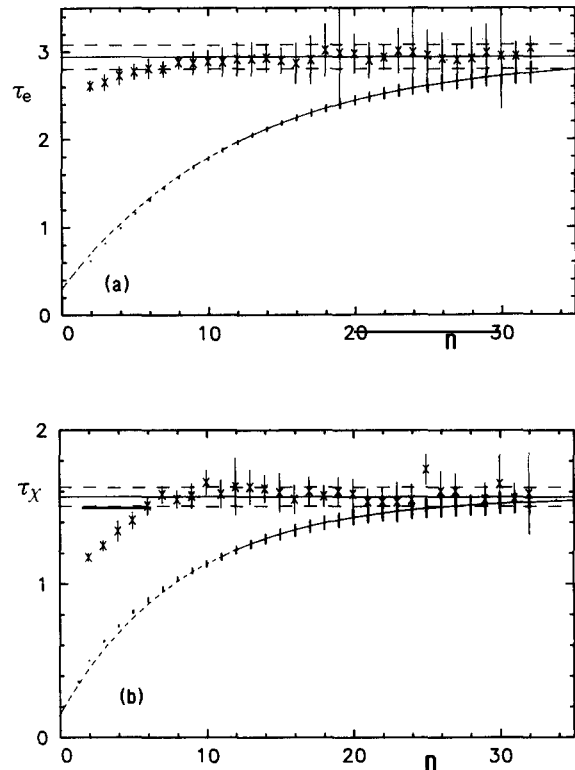


Fig. 1. Integrated autocorrelation times (thick vertical bars) for (a) the energy and (b) the susceptibility versus the upper summation limit  $n$  at  $\beta_0 = 0.4539$  on a  $32^3$  lattice. The solid line interpolating the data is a fit (for  $n \geq 12$ ) to the right-hand side of eq. (7), and the crosses are the improved extrapolants according to eq. (8). The fitted values of  $\tau_e$  and  $\tau_\chi$  and their errors are displayed by the horizontal solid and dashed lines, respectively.

ferent. It increases with lattice size, and a rough fit gives

$$\tau_e \approx 1.3L^{0.25}. \quad (11)$$

The data labeled "SW" show the corresponding results of ref. [21] for the multiple cluster Swendsen-Wang update. Compared with the single cluster update the SW correlation times  $\tau \propto L^z$  are growing obviously much faster with  $L$ , and are larger in magnitude for all lattice sizes (this is of course what really matters – a constant  $\tau = 100$ , say, would not really help, even though the exponent  $z$  is reduced to zero). We can thus conclude that for the three-dimensional XY model the *single* cluster update is more efficient than the *multiple* cluster SW algorithm, which is, of

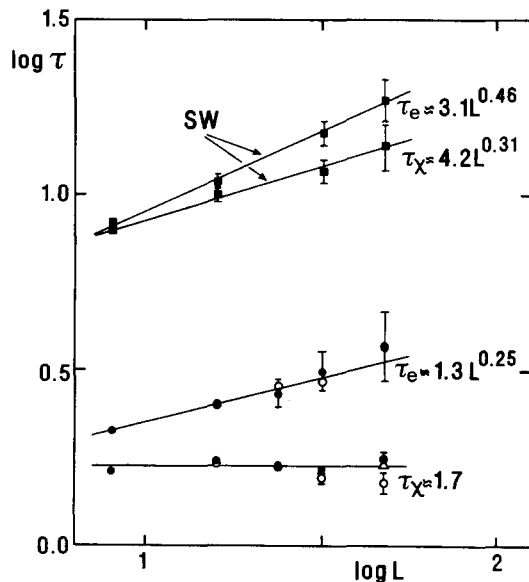


Fig. 2. Double logarithmic plot of the integrated autocorrelation times near criticality ( $(\circ)$   $\beta_0=0.4539$ ,  $(\bullet)$   $\beta_0=0.4543$ ,  $(\Delta)$   $\beta_0=0.45415$ ) versus the linear size of the lattice,  $L$ . The data labeled "SW" are taken from ref. [21] ( $\beta=0.45421$ ), employing the multiple cluster Swendsen-Wang update.

course, already a significant improvement on the by now "old fashioned" local Metropolis update.

Using the single cluster update, it is possible to calculate physical quantities like critical exponents in reasonable computer times with an accuracy comparable to the currently best estimates coming from field theoretic approaches (Borel resummed perturbation series or  $\epsilon$ -expansions). In order to increase the efficiency of the MC method further, we have supplemented the single cluster update by using improved estimators for measurements and histogram sampling for their analyses. For the susceptibility, the improved estimator is given by [8]

$$\chi^{\text{imp}} = 2 \left\langle C \left( \frac{1}{C} \sum_{x \in \mathcal{C}} \mathbf{r} \cdot \mathbf{s}(x) \right)^2 \right\rangle, \quad (12)$$

where  $\mathbf{r}$  is the unit vector defining the (orthogonal) mirror line, and  $x$  runs over all sites belonging to the cluster  $\mathcal{C}$  of size  $C$ . For large lattices and away from criticality, the statistical errors of  $\chi^{\text{imp}}$  are much smaller than those of  $\chi$  in eq. (3). Near criticality, however, there is no advantage in using (12) instead of (3).

The histogram sampling technique [23], on the

other hand, works best near criticality and is in this sense thus complementary to the use of improved estimators. It is a quite general technique of data analysis based on the simple idea of recording whole distribution functions, and not only their first and second moments (e.g., the average energy and specific heat), as is usually done. The energy histogram (normalized to unit area) at  $\beta_0$  can be written as

$$P_{\beta_0}(E) \Delta E = N(E) \Delta E \exp(-\beta_0 E) / Z(\beta_0), \quad (13)$$

where  $N(E) \Delta E$  is the number of states with energy in the interval  $E - (E + \Delta E)$ . It is then easy to see that an expectation value  $\langle f(E) \rangle$  can in principle be calculated for any  $\beta$  from

$$\begin{aligned} \langle f(E) \rangle(\beta) &= \frac{\int_0^\infty dE f(E) P_{\beta_0}(E) \exp[-(\beta - \beta_0)E]}{\int_0^\infty dE P_{\beta_0}(E) \exp[-(\beta - \beta_0)E]}. \end{aligned} \quad (14)$$

Clearly, in practice the wings of  $P_{\beta_0}(E)$  have large statistical errors, and (14) gives reliable results only for  $\beta$  near  $\beta_0$ . If  $\beta_0$  is near criticality, the distribution is quite broad and the method works best. In this case reliable estimates from (14) can be expected for  $\beta$  values in an interval around  $\beta_0$  of width  $\propto L^{-1/\nu}$ , i.e., just in the finite-size scaling region.

We have used this histogram sampling technique to find the  $\beta$  dependence of the fourth-order cumulant [24],

$$U(\beta) = 1 - \frac{1}{3} \frac{\langle (m^2)^2 \rangle}{\langle m^2 \rangle^2}, \quad (15)$$

from two simulations at  $\beta_0=0.4539$  and  $\beta'_0=0.4543$  (for each lattice size). It is well known [24] that the  $U(\beta)$  curves for different  $L$  cross around  $(\beta_c, U^*)$  with slopes  $\propto L^{1/\nu}$  (apart from confluent corrections explaining small systematic deviations). This allows an almost unbiased estimate of  $\beta_c$ ,  $U^*$ , and the critical exponent  $\nu$ . The  $U(\beta)$  curves calculated from the histograms at  $\beta_0=0.4539$  and  $\beta'_0=0.4543$  are shown in fig. 3 as solid and dashed lines, respectively. In the critical region, they lie practically on top of each other. Using their average #2 for the final analysis (and taking into account the confluent corrections [27]), we obtain from the crossing points

#2 Since the accuracy of both curves is comparable, more refined averaging procedures [25,26] are not necessary.

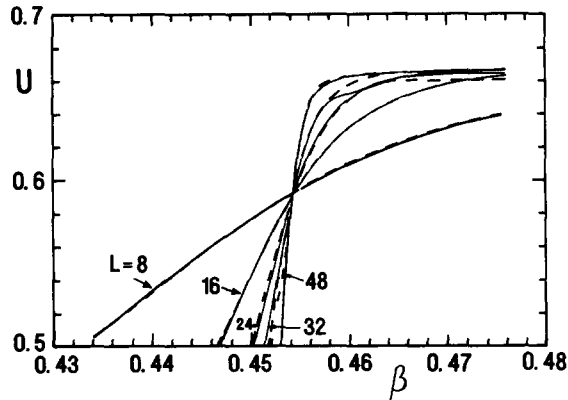


Fig. 3. Fourth order cumulant  $U$  versus  $\beta$ . The curves are calculated from histograms at  $\beta_0=0.4539$  (solid lines) and  $\beta_0=0.4543$  (dashed lines). The crossing point locates  $\beta_c=0.4542 \pm 0.0001$ .

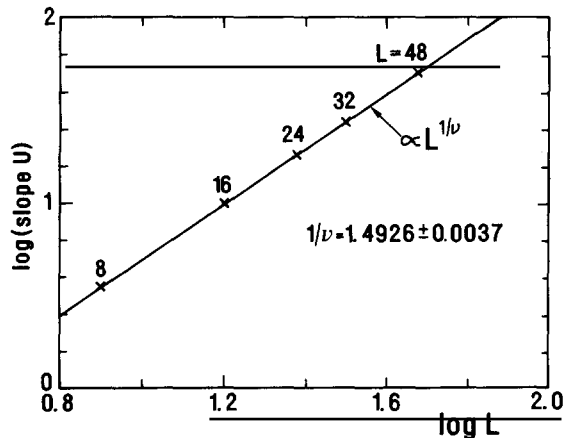


Fig. 4. The slopes of  $U$  in fig. 3 near the crossing point versus  $L$  in a double logarithmic plot. The slope of the linear least-square fit gives an estimate for the critical exponent  $\nu$ .

$$\beta_c = 0.4542 \pm 0.0001, \quad (16)$$

$$U^* = 0.586 \pm 0.001, \quad (17)$$

and from the slope of the slopes of  $U$  versus  $L$  in the double logarithmic representation of fig. 4 we read off

$$\nu = 0.670 \pm 0.002. \quad (18)$$

For comparison, field theoretical estimates are  $U^*=0.5518$  ( $\sqrt{\epsilon}$ -expansion [28]), and  $\nu=0.669 \pm 0.002$  (resummed perturbation series [29]),  $\nu=0.671 \pm 0.005$  (resummed  $\epsilon$ -expansion [30]).

To compare with the recent MC simulation by Li and Teitel [20], we have also measured the helicity modulus [31],

$$Y_i = \left\langle \frac{1}{V} \sum_{\mathbf{x}} \mathbf{s}(\mathbf{x}) \cdot \mathbf{s}(\mathbf{x}+i) \right\rangle - \beta \left\langle \frac{1}{V} \left( \sum_{\mathbf{x}} [s_y(\mathbf{x})s_x(\mathbf{x}+i) - s_x(\mathbf{x})s_y(\mathbf{x}+i)] \right)^2 \right\rangle, \quad (19)$$

which is proportional to the superfluid density and thus of direct physical importance. Another motivation comes from the recent phenomenological renormalization group predictions for this quantity [19]. The solid lines in fig. 5 show our results for  $Y \equiv \sum_i Y_i/3$  near  $T_c$ . Each line is an average of two curves, calculated from the histograms of the simulations at  $\beta_0=0.4539$  and  $\beta_0=0.4543$ . For  $L=4, 8,$

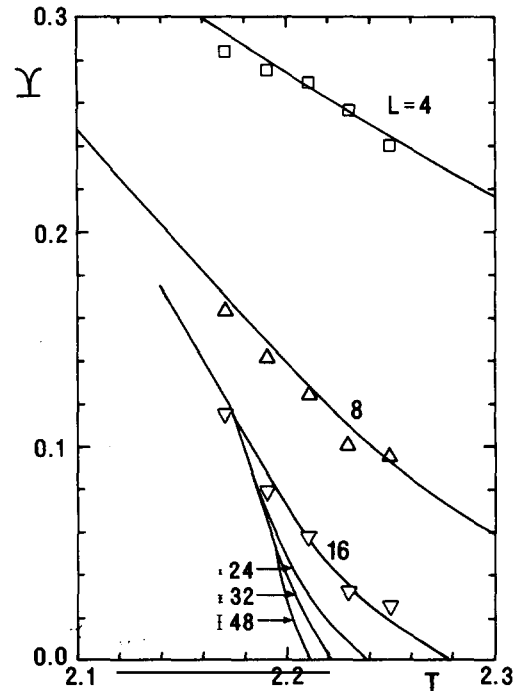


Fig. 5. Helicity curves near  $T_c$  calculated from histograms at  $\beta_0=0.4539$  and  $\beta_0=0.4543$  versus temperature. For  $L=4, 8,$  and  $16$ , the errors are of the thickness of the lines, and for  $L=24, 32,$  and  $48$ , their order of magnitude is indicated by the vertical bars. For comparison also the less accurate data points ( $\square, \triangle, \nabla$ ) from ref. [20] are shown.

16, they are clearly much more accurate than the data in ref. [20] which are shown for comparison. Following the finite-size scaling analysis in ref. [20], also  $\chi$  can be used to derive estimates of  $\beta_c$  and  $\nu$  which, however, turn out to be less accurate than (16) and (18) [27].

In order to estimate the exponent  $\gamma$ , we have measured the susceptibility also in the high-temperature phase down to  $\beta=0.40$ , using the improved estimator (12). Performing a (non-linear) three parameter fit [22] of our data on  $32^3$  and  $48^3$  lattices compiled in table 1 to the form

$$\chi = \chi_+ (\beta_c - \beta)^{-\gamma}, \quad (20)$$

we get (omitting the point at  $\beta=0.45$ , which requires still larger lattices)

$$\beta_c = 0.45408 \pm 0.00008, \quad (21)$$

$$\chi_+ = 0.363 \pm 0.005, \quad (22)$$

$$\gamma = 1.316 \pm 0.005. \quad (23)$$

Notice that this estimate of  $\beta_c$  is somewhat smaller, but still consistent with the value in (16), determined from the fourth order cumulant. In order to get an estimate of the systematic dependence of  $\gamma$  on  $\beta_c$ , we have performed (linear) two parameter fits with fixed  $\beta_c$  also. At the earlier estimate  $\beta_c=0.4542$ , we obtain  $\chi_+ = 0.356 \pm 0.002$  and  $\gamma = 1.323 \pm 0.002$ , and recover (21)–(23) as the fit with the best “goodness”  $Q \approx 0.9$  (relying on the subroutine FIT of

ref. [22]). The purely statistical errors of these fits are smaller because the parameter  $\beta_c$  is fixed. Adding the systematic errors due to the variation in  $\beta_c$ , we recover roughly the error estimates in (22) and (23). This and other tests confirm that the ansatz (20) is a good approximation for the lattice sizes and the  $\beta$  interval we have used for the fits. For comparison, from high-temperature expansions<sup>#3</sup> we know that  $\chi_+ = 0.362 \pm 0.018$  [12], and the field theory estimates are  $\gamma = 1.316 \pm 0.0026$  (resummed perturbation series [29]),  $\gamma = 1.315 \pm 0.007$  (resummed  $\epsilon$ -expansion [30]).

Finally, using the scaling relation  $\gamma/\nu = 2 - \eta$ , we can estimate  $\eta = 0.036 \pm 0.014$ . Fitting our data at criticality to  $\chi \propto L^{\nu/\nu}$ , we find the lower value  $\eta \approx 0.02$ . The latter estimate is, however, very sensitive to the precise value of  $\beta_c$  [27]. The field theory values are  $\eta = 0.031 \pm 0.004$  (resummed perturbation series [29]),  $\eta = 0.040 \pm 0.003$  (resummed  $\epsilon$ -expansion [30]).

In conclusion we have shown that the single cluster update eliminates critical slowing down in the three-dimensional XY model almost completely, and that it is more efficient than the multiple cluster Swendsen–Wang algorithm. Combined with improved estimators and the histogram sampling method this allows a precise Monte Carlo determination of critical indices in three dimensions (in rea-

<sup>#3</sup> Notice the different normalizations,  $\chi = 2\chi^{\text{HTS}}$ .

Table 1

Results for energy ( $e$ ), specific heat ( $c$ ), and susceptibility ( $\chi, \chi^{\text{imp}}$ ) of the single cluster simulations in the high-temperature phase.  $N$  is the number of measurements taken every  $N_0$  update steps, and “moved” denotes the fraction  $\langle C \rangle N_0 / V$  of moved spins between measurements.

$\beta$	$L$	$N$	$N_0$	Moved	$e$	$c$	$\chi$	$\chi^{\text{imp}}$
0.40	32	150000	50	0.0212	2.25901(15)	0.503(10)	16.98(12)	16.887(18)
0.40	48	75000	50	0.00632	2.25917(20)	0.515(29)	16.31(31)	16.849(26)
0.41	32	15000	800	0.442	2.22667(17)	0.559(11)	22.13(17)	22.101(22)
0.42	32	15000	600	0.463	2.19123(17)	0.666(13)	30.98(22)	30.978(40)
0.43	32	20000	400	0.487	2.15131(16)	0.789(11)	48.37(37)	49.020(84)
0.435	48	120000	50	0.0245	2.12948(13)	0.845(22)	66.50(41)	66.60(13)
0.44	32	40000	135	0.333	2.10521(18)	0.983(13)	98.60(50)	99.50(27)
0.44	48	50000	50	0.364	2.10592(24)	1.018(37)	98.00(89)	99.15(35)
0.445	32	40000	100	0.433	2.07842(18)	1.190(16)	175.97(96)	174.81(62)
0.445	48	110000	50	0.0649	2.07880(12)	1.086(19)	178.04(83)	176.88(47)
0.45	32	25000	50	0.534	2.04455(27)	1.637(30)	432.1(3.4)	431.4(2.9)
0.45	48	10000	145	0.518	2.04727(20)	1.538(32)	488.5(4.9)	487.6(3.5)

sonable computer times), whose accuracy is comparable with the best estimates coming from field theoretical methods. The details of our numerical analyses as well as numerical tables will be given elsewhere [27].

The author thanks Professor W. Theis for a useful discussion.

## References

- [1] K. Binder, in: Monte Carlo methods in statistical physics, ed. K. Binder (Springer, Berlin, 1979) p. 1; V. Privman, ed., Finite-size scaling and numerical simulations of statistical systems (World Scientific, Singapore, 1990).
- [2] M. Creutz, Phys. Rev. D 36 (1987) 515; R. Gupta, J. DeLapp, G.G. Battrouni, G.C. Fox, C.F. Baillie and J. Apostolakis, Phys. Rev. Lett. 61 (1988) 1996; S.L. Adler, Phys. Rev. D 37 (1988) 458; H. Neuberger, Phys. Lett. B 207 (1988) 461.
- [3] D. Kandel, E. Domany, D. Ron, A. Brandt and E. Loh Jr., Phys. Rev. Lett. 60 (1988) 1591; D. Kandel, E. Domany and A. Brandt, Phys. Rev. B 40 (1989) 330.
- [4] R.H. Swendsen and J.S. Wang, Phys. Rev. Lett. 58 (1987) 86.
- [5] U. Wolff, Phys. Rev. Lett. 62 (1989) 361; Nucl. Phys. B 322 (1989) 759.
- [6] R.G. Edwards and A.D. Sokal, Phys. Rev. D 40 (1989) 1374.
- [7] U. Wolff, Phys. Lett. B 222 (1989) 473.
- [8] U. Wolff, DESY preprint 89-021 (1989).
- [9] U. Wolff, Phys. Lett. B 228 (1989) 379.
- [10] V.G. Vaks and A.I. Larkin, Zh. Eksp. Teor. Fiz. 49 (1965) 975 [Sov. Phys. JETP 22 (1966) 678]; R.G. Bowers and G.S. Joyce, Phys. Rev. Lett. 19 (1967) 630.
- [11] P.L. Kapitza, Nature 141 (1937) 74; Zh. Eksp. Teor. Fiz. 11 (1941) 1.
- [12] M. Ferer, M.A. Moore and M. Wortis, Phys. Rev. B 8 (1973) 5205.
- [13] R. Savit, Rev. Mod. Phys. 52 (1980) 453.
- [14] H. Kleinert, Gauge fields in condensed matter (World Scientific, Singapore, 1989).
- [15] L. Onsager, Nuovo Cimento Suppl. 6 (1949) 249.
- [16] R.P. Feynman, Prog. Low Temp. Phys. 1 (1955) 17.
- [17] E. Byckling, Ann. Phys. 32 (1965) 367; V.N. Popov, Zh. Eksp. Teor. Fiz. 64 (1973) 672 [Sov. Phys. JETP 37 (1973) 341]; F.W. Wiegel, Physica 65 (1973) 321; Phys. Rep. 16 (1975) 58; Introduction to path integral methods in physics and polymer science (World Scientific, Singapore, 1986).
- [18] N. Gupte and S.R. Shenoy, Phys. Rev. D 33 (1986) 3002; G.A. Williams, Phys. Rev. Lett. 59 (1987) 1926; 61 (1988) 1142(E); S.R. Shenoy, Phys. Rev. B 40 (1989) 5056.
- [19] G.A. Williams, UCLA preprint, to appear in: Proc. LT19 (1990).
- [20] Y.-H. Li and S. Teitel, Phys. Rev. B 40 (1989) 9122.
- [21] M. Hasenbusch and S. Meyer, preprint KL-TH 11/89, Kaiserslautern (1989).
- [22] W.H. Press, B.P. Flannery, S.A. Teukolsky and W.T. Vetterling, Numerical recipes - The art of scientific computing (Cambridge Univ. Press, Cambridge, 1986).
- [23] A.M. Ferrenberg and R.H. Swendsen, Phys. Rev. Lett. 61 (1988) 2635.
- [24] K. Binder, Z. Phys. B 43 (1981) 119.
- [25] A.M. Ferrenberg and R.H. Swendsen, Phys. Rev. Lett. 63 (1989) 1195; Int. J. Mod. Phys. D 1 (1990), to be published.
- [26] P.B. Bowen, J.L. Burke, P.G. Corsten, K.J. Crowell, K.L. Farrell, J.C. MacDonald, R.P. MacDonald, A.B. MacIsaac, P.H. Poole and N. Jan, Phys. Rev. B 40 (1989) 7439.
- [27] W. Janke, to be published.
- [28] E. Brézin and J. Zinn-Justin, Nucl. Phys. B 257 [FS14] (1985) 867.
- [29] J.C. Le Guillou and J. Zinn-Justin, Phys. Rev. B 21 (1980) 3976.
- [30] J.C. Le Guillou and J. Zinn-Justin, J. Phys. Lett. (Paris) 46 (1985) L137.
- [31] T. Ohta and D. Jasnow, Phys. Rev. B 20 (1979) 139; S. Teitel and C. Jayaprakash, Phys. Rev. B 27 (1983) 589.